



## Enhanced anode performance of microbial fuel cells by adding nanosemiconductor goethite

Xinhong Peng <sup>a,b,c</sup>, Hongbing Yu <sup>a,b,c,\*,1</sup>, Xin Wang <sup>a,b,c,\*,1</sup>, Ningshengjie Gao <sup>a,b,c</sup>, Lijuan Geng <sup>a,b,c</sup>, Lina Ai <sup>a,b,c</sup>

<sup>a</sup> MOE Key Laboratory of Pollution Processes and Environmental Criteria, College of Environmental Science and Engineering, Nankai University, No. 94 Weijin Road, Nankai District, Tianjin 300071, China

<sup>b</sup> Tianjin Key Laboratory of Environmental Remediation and Pollution Control, College of Environmental Science and Engineering, Nankai University, No. 94 Weijin Road, Nankai District, Tianjin 300071, China

<sup>c</sup> Research Center for Cleaner Production, College of Environmental Science and Engineering, Nankai University, No. 94 Weijin Road, Nankai District, Tianjin 300071, China

### HIGHLIGHTS

- Anodes are made by rolling  $\alpha$ -FeOOH into activated carbon on stainless steel mesh.
- The addition of  $\alpha$ -FeOOH in anode increases the maximum power density by 36%.
- $\alpha$ -FeOOH in the anode accelerated the extracellular electron transfer.
- Excess  $\alpha$ -FeOOH resulted in the decay of performance.

### ARTICLE INFO

#### Article history:

Received 6 August 2012

Received in revised form

14 September 2012

Accepted 15 September 2012

Available online 21 September 2012

#### Keywords:

Microbial fuel cells

Nanosemiconductor goethite

Extracellular electron transfer

Bioelectrochemical systems

### ABSTRACT

Nano goethite with contents of 0, 2.5%, 5.0% and 7.5% (mass percentage) were added into activate carbon powder (AC) and rolled onto stainless steel mesh to fabricate new anodes for microbial fuel cells (MFCs). The maximum power density of MFC with 5.0%  $\alpha$ -FeOOH ( $693 \pm 20 \text{ mW m}^{-2}$ ) is 36% higher than that of the AC control ( $508 \pm 40 \text{ mW m}^{-2}$ ). Based on the decrease of charge transfer resistance and the increases of both exchange current density and anodic peak current in electrochemical impedance and polarization tests, the addition of nano  $\alpha$ -FeOOH kinetically promotes the extracellular electron transfer between bacteria and the electrode. The increase of constant-phase element and the decrease of Warburg element show that  $\alpha$ -FeOOH enhances both the capacitance and diffusion condition on the surface of anode. However, the excess  $\alpha$ -FeOOH of 7.5% incurs a negative effect on surface conductivity, capacitance and diffusion, probably due to the adsorption of biogenic Fe(II) on the anodic surface.

© 2012 Elsevier B.V. All rights reserved.

## 1. Introduction

Microbial fuel cell (MFC) is a promising technology for wastewater treatment and bioenergy production [1]. Various novel MFCs have been developed to produce hydrogen (microbial

electrolysis cells, MECs [2]), to desalinate water (microbial desalination cells, MDCs [3,4]), or to power wireless sensors [5]. All these bioelectrochemical systems share the key feature that the electron transfer from organic matter to electrodes (anodes) is catalyzed by bacteria. Therefore, improving the anodic performance is critical for the future application of MFCs [6]. Among those factors related with anode performance, anode material plays an important role. To enhance the anodic performance, exogenous electron shuttles such as AQDS, quinone, humic acid and neutral red have been used to facilitate indirect electron transfer to anode [7,8]. However, these mediators are usually expensive, toxic and easily washed away, resulted in extra operational losses [9]. Therefore, to accelerate the direct electron transfer on anode is much more significant [10,11].

\* Corresponding author. MOE Key Laboratory of Pollution Processes and Environmental Criteria, College of Environmental Science and Engineering, Nankai University, No. 94 Weijin Road, Nankai District, Tianjin 300071, China.

\*\* Corresponding author. Research Center for Cleaner Production, College of Environmental Science and Engineering, Nankai University, No. 94 Weijin Road, Nankai District, Tianjin 300071, China. Tel./fax: +86 22 23502756.

E-mail addresses: [hongbingyu1130@sina.com](mailto:hongbingyu1130@sina.com) (H. Yu), [xinwang1@nankai.edu.cn](mailto:xinwang1@nankai.edu.cn) (X. Wang).

<sup>1</sup> These authors contributed equally to this work.

The exoelectrogenic bacteria in MFCs, which mainly consist of dissimilatory metal-reducing bacteria (DIRB), like *Shewanella* and *Geobacter* species, are able to transport respiratory electron and conserve energy [12]. This type of electron transfer, named extracellular electron transfer (EET), has currently attracted considerable attention. Electrons obtained from anaerobic oxidation are delivered from inner membrane to periplasm and outer membrane through electron transport proteins, such as c-type cytochromes (c-Cyts), toward the anode surface [13]. It has been experimentally demonstrated that outer membrane c-type cytochromes (OM c-Cyts) have a high binding affinity to Fe(III) oxide [14,15]. Furthermore, Fe(III) oxide can be recognized by DIRB [16] and utilized as electron shuttle to reduce distant terminal acceptors [17,18]. The role of OM c-Cyts for respiratory Fe(III) oxide reduction has also been suggested by Mehta et al. [19] and Xiong et al. [15]. Lowy et al. [8] found that the modification of anode by  $\text{Fe}_3\text{O}_4$  enhanced the kinetic activity by 120% compared to that of the unmodified anode in sediment MFCs. Ji et al. [20] also reported that the  $\text{Fe}_2\text{O}_3$  electrode prepared by layer-by-layer self-assembly technique can be used as the anode to produce 320% enhancement comparing with the bare anode. Our previous study [21] illustrated that the addition of nano  $\text{Fe}_3\text{O}_4$  to anodes enhanced the power density by 22% from  $664 \pm 17 \text{ mW m}^{-2}$  to  $809 \pm 5 \text{ mW m}^{-2}$ , probably due to the improvement of both kinetic activity and capacitance.

Currently, nanostructure materials have received more and more attention as promising anodes of MFCs [22–24]. Here we fabricated an activated carbon powder (AC)/nano  $\alpha$ -FeOOH/stainless steel mesh (SSM) composite anode for power generation. The SSM was utilized as both matrix and current collector. The goethite ( $\alpha$ -FeOOH), an iron oxide with lower solubility in water than magnetite [25] and hematite [26], was functioned mainly as a promoter for EET acceleration. The effect of  $\alpha$ -FeOOH content on MFC performance was investigated and the mechanisms were also discussed based on bio-electrochemical tests.

## 2. Materials and methods

### 2.1. Preparation of $\alpha$ -FeOOH

All reagents were analytical grade and were used without further purification. Manipulations and reactions were carried out in air without the protection of nitrogen or other inert gas. In a typical synthesis, 2.1 g of  $\text{FeSO}_4 \cdot 7\text{H}_2\text{O}$  was dissolved into 18 mL of 30 wt %  $\text{H}_2\text{O}_2$  under stirring for 20 min. After that, the mixture was transferred into a 50 mL Teflon-lined autoclave, sealed, and then heated to 150 °C for 6 h. After being cooled down to room temperature naturally, the products were collected by centrifugation and sequentially washed with deionized water and ethanol several times. Finally, the products were dried under vacuum at 80 °C for further application.

### 2.2. Preparation of MFCs anodes

The anodes were prepared according to the following procedures.  $\alpha$ -FeOOH and AC powder were mixed with mass percentage of 0, 2.5%, 5.0% and 7.5% of  $\alpha$ -FeOOH, dispersed into 25 mL of ethanol for each sample, and 33  $\mu\text{L}$  polytetrafluoroethylene (PTFE; 60 wt %; Horizon Ltd, Shanghai, China) per gram mixture was added drop by drop under a water bath of 80 °C. When the mixture became a homogeneous doughlike paste, it was roll-pressed into a sheet with 0.2 mm in thickness as previously described [21,27]. Finally, the sheet was roll-pressed onto a SSM (type 304L, 80 × 80, thickness of 0.2 mm) current collector. The prepared anodes were finally cut into circles with the diameter of 4 cm for the following utilization in MFCs.

### 2.3. MFC setup and operation

Each membrane-less single chambered MFC was fabricated with a total volume of 28 mL as described by Liu and Logan [28]. The prepared electrodes with different  $\alpha$ -FeOOH contents were used as MFC anodes with the Fe-free anode as the control. Air-cathode was made of carbon mesh (10 wt % wet proof, Jilin Carbon Plant Co. Ltd, China) with four PTFE diffusion layers and 0.5 mg  $\text{cm}^{-2}$  platinum loaded as catalyst according to Wang et al. [29]. Anode and cathode were connected to a 1 k $\Omega$  resistor (except as noted) using titanium wire with an electrode spacing of 4 cm.

MFCs were initially inoculated using a pre-acclimated cell suspension from MFCs fed with acetate for 3 months and operated in batch mode. The inoculation was switched into 50 mM phosphate buffer solution (PBS) medium until the cell voltage was higher than 300 mV. MFC was considered for testing when similar cell voltage was produced over three consecutive cycles. The PBS medium contains (g  $\text{L}^{-1}$ ):  $\text{Na}_2\text{HPO}_4$  4.576,  $\text{NaH}_2\text{PO}_4 \cdot \text{H}_2\text{O}$  3.321,  $\text{NH}_4\text{Cl}$  0.31,  $\text{KCl}$  0.13, trace minerals and vitamins [30] and 1 g  $\text{L}^{-1}$  sodium acetate. All the reactors were operated in a  $30 \pm 0.5^\circ\text{C}$  temperature-controlled biochemical incubator in duplicate.

### 2.4. Analysis

The voltages across resistors were recorded every 30 min using a data acquisition system (PISO-813, ICP DAS Co., Ltd.). Anode and cathode potentials were obtained using Ag/AgCl as reference electrode (+197 mV, saturated KCl, versus standard hydrogen electrode; SHE). Polarization and power density curves were obtained by changing resistances over a range from 1000 to 50  $\Omega$ . The power density  $P$  ( $\text{mW m}^{-2}$ ) was calculated according to  $P = IV/A$ . The relative decrease in anode potential (RDAP) is the function of the applied external resistance. Under high external resistance, the current is limited by the external resistance, and the RDAP increases linearly with the decrease of external resistance. At low external resistance, the electron delivered to the cathode is limited by kinetic and/or mass transfer, and the RDAP increases linearly with different slopes. Once the external and internal resistance limitations are equal, a horizontal line from the intersection drew to obtain the sustainable resistance and evaluate the sustainable power output [31].

The bio-electrochemical measurements were conducted *in situ* by employing an electrochemical workstation (CHI660D, CH Instruments Inc., China) in a single chambered MFC reactor, with the anode as the working electrode, the cathode as the counter electrode, and an Ag/AgCl as the reference electrode. Electrochemical impedance system (EIS) measurements were performed at the open circuit potentials with the voltage amplitude of 5 mV over the frequency range from 100 kHz to 0.01 Hz. The EIS data are simulated by Zsimpwin software (ver. 3.10). The equivalent circuit model (ECM) is proposed in Fig. 1 with the assumption that the anode reaction is affected by both reaction kinetics and diffusion.

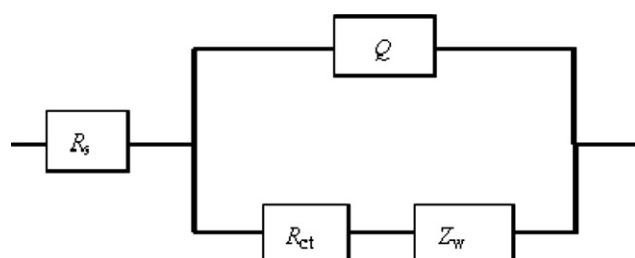


**Fig. 1.** The proposed equivalent circuit for simulation of EIS results.

The parameter  $R_s$  represents the solution resistance, and  $R_{ct}$  is the charge transfer resistance.  $Q$  is the constant-phase element (CPE) with two parameters,  $Q_{dl}$  and  $N$ , where  $Q_{dl}$  describes the non-ideal capacitance behavior distributed along the pores of the anodic surface, and  $N$  is used as a gauge of surface heterogeneity.  $Z_w$  is Warburg impedance. Tafel measurement explains the kinetics of the electrode reaction with different  $\alpha$ -FeOOH content. Tafel plot was recorded by sweeping voltage at  $1 \text{ mV s}^{-1}$  from the open circuit potential (OCP) of the anode (versus Ag/AgCl) to an overpotential of  $\pm 80 \text{ mV}$  [8]. Tafel equation for anodic oxidation and reduction can be expressed as follows:

$$\ln i = \ln i_0 + \alpha n F \eta / RT \quad (1)$$

$$\ln i = \ln i_0 - \beta n F \eta / RT \quad (2)$$

where  $\eta$  is the activation overpotential (mV),  $R$  is the universal gas constant ( $8.314 \text{ J mol}^{-1} \text{ K}^{-1}$ ),  $T$  is the absolute temperature (K),  $\alpha$  and  $\beta$  are the oxidative and reductive transfer coefficient,  $n$  is the number of electrons transferred at the rate determining step,  $F$  is the Faraday constant ( $96,485 \text{ C mol}^{-1}$ ),  $i$  is the current density ( $\text{A cm}^{-2}$ ) and  $i_0$  is the exchange current density ( $\text{A cm}^{-2}$ ). Since  $(\alpha + \beta)$  is equal to  $n$ , Tafel slope and intercept,  $i_0$  and  $n$  can be calculated from the equations above. The kinetic activity (KA) of each anode was calculated by normalizing the  $i_0$  to that of the Fe-free control [8]. Cyclic voltammetry (CV) response of the biofilm was recorded under acetate saturation condition. CV was performed by applying a potential ramp at a scan rate of  $0.1 \text{ mV s}^{-1}$  over the potential range from  $-0.8$  to  $0 \text{ V}$  (versus Ag/AgCl). First derivative of CV (DCV) was derived from the CV data.

### 3. Results and discussion

#### 3.1. Effect of $\alpha$ -FeOOH content on power generation

Different electrodes, added with different contents of  $\alpha$ -FeOOH (0, 2.5%, 5.0% and 7.5%) were simultaneously implemented as anodes in MFCs. The cell voltages increased from  $<10 \text{ mV}$  to ca.  $500$ – $530 \text{ mV}$  for all MFCs during 20 days, with no remarkable difference observed on the startup time. A few amount of Fe was observed ( $<2 \text{ mg L}^{-1}$ ) during the start-up period, indicating that the Fe leakage was neglectable compared to the total amount of Fe. As showed in Fig. 2A, the polarization data demonstrated that the maximum power density (MPD) was significantly increased after  $\alpha$ -FeOOH addition. The MPD increased by 36% from  $508 \pm 40 \text{ mW m}^{-2}$  (the control) to a maximum of  $693 \pm 20 \text{ mW m}^{-2}$  when 5.0%  $\alpha$ -FeOOH was added into anode. Increase or decrease of the  $\alpha$ -FeOOH content to 7.5% or 2.5% resulted in decrease in MPD to  $639 \pm 30 \text{ mW m}^{-2}$  or  $637 \pm 51 \text{ mW m}^{-2}$ .

The electrode potentials (Fig. 2B) showed that the differences in MPDs were attributed to the performance of anodes but not cathodes. The most negative anode potential was achieved with the 5.0%  $\alpha$ -FeOOH added anode, followed by 7.5%, 2.5% and the control at the same current density, with these differences increased at higher current densities. It was noted that the performance of anode was enhanced when  $\alpha$ -FeOOH was initially added (2.5%) and increased (5.0%), however, the further increment in  $\alpha$ -FeOOH content did not result in a correspondent improvement on anode performance. This phenomenon was also confirmed by the following bio-electrochemical tests.

When the external resistance varied from 10 to 0.5 k $\Omega$ , the lowest increase rate of 35% in RDAP (Fig. 3) was obtained for 5.0%  $\alpha$ -FeOOH added anode, followed by 43% and 45% for the anodes with  $\alpha$ -FeOOH contents of 7.5% and 2.5%, while 50% for the control,

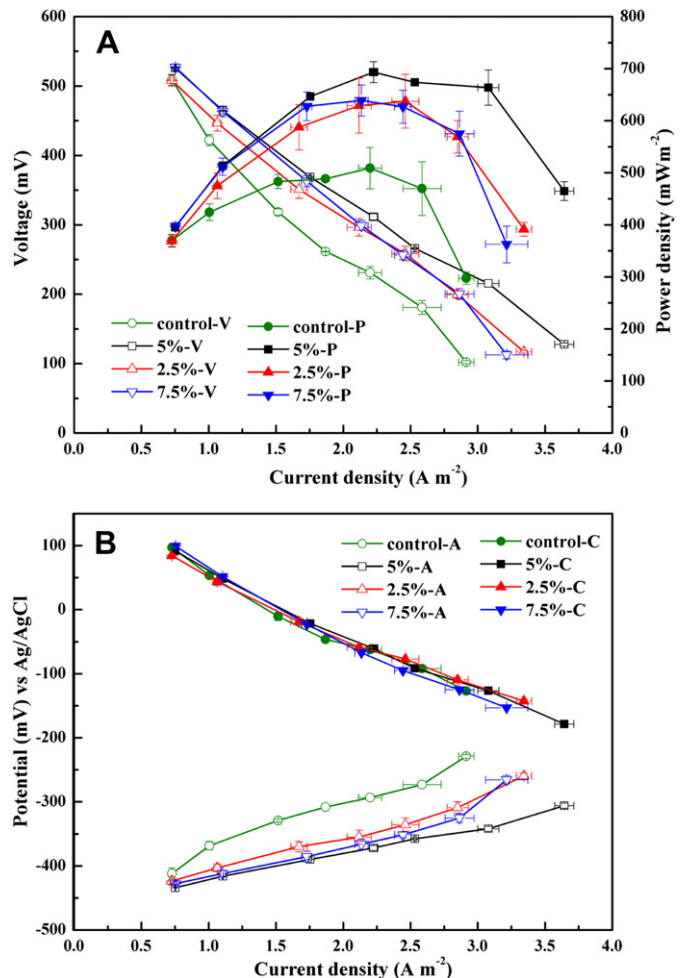
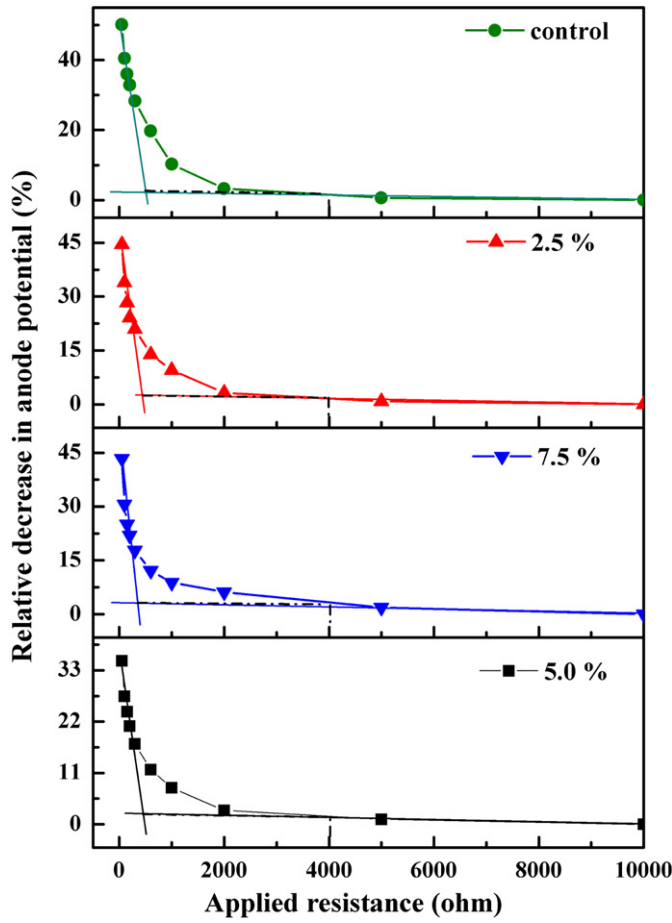


**Fig. 2.** Polarization and power density curves (A) and electrode potential curves (B) of MFCs using anodes with different  $\alpha$ -FeOOH contents. Error bars  $\pm \text{SD}$  were based on averages measured in duplicate.

indicating that the addition of  $\alpha$ -FeOOH reduced the activation overpotential of cell metabolism at high external resistance. This was in accordance with the results from polarization curves. When the power generated by the MFC equals to the power consumption for an extended time, the MFC system is at a steady state where the power generation is sustainable [31]. Fig. 3 illustrated that all the MFCs had similar sustainable resistance of  $4000 \Omega$  in concurrence with similar voltage output of  $635 \pm 2 \text{ mV}$ , and with corresponding sustainable power densities of  $144 \pm 1.5 \text{ mW m}^{-2}$ , indicating that the addition of  $\alpha$ -FeOOH had no effect on the sustainable power output.

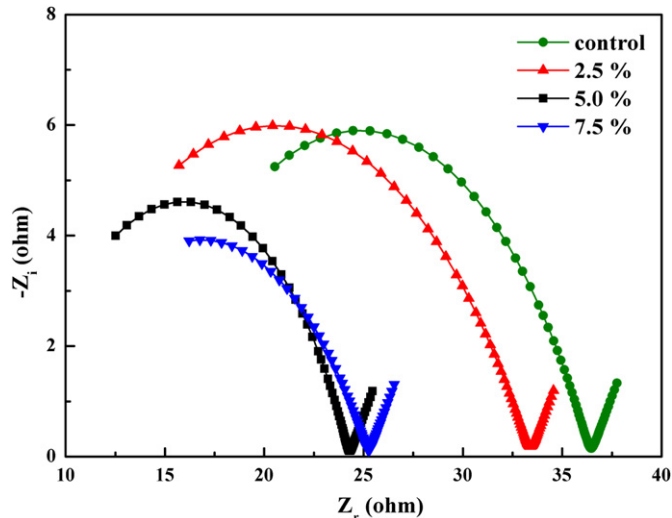
#### 3.2. EIS analysis

Fig. 4 shows the typical (both experimental and modeled) Nyquist impedance spectra of anodes with different  $\alpha$ -FeOOH contents after the MFCs were stable, where the independent axis is the real impedance ( $Z_R(\Omega)$ ) and the dependent axis is the imaginary impedance ( $-Z_i(\Omega)$ ). All the parameters were reasonable values with fit errors of  $\leq 10\%$ . As showed in Table 1, the internal resistances decreased after  $\alpha$ -FeOOH addition. It was showed that  $R_s$  and  $R_{ct}$  decreased by 25% ( $7.6 \Omega$ ) and 37% ( $16.6 \Omega$ ) for 5.0%  $\alpha$ -FeOOH added anode than those of the control ( $10.2$  and  $26.2 \Omega$ ). Increase or decrease of  $\alpha$ -FeOOH content to 7.5% or 2.5% resulted in both decrease for  $R_s$  and



**Fig. 3.** The relative decrease in anode potential of MFCs with different  $\alpha$ -FeOOH contents.

$R_{ct}$  to 8.4 and 16.8  $\Omega$  or 7.7 and 25.6  $\Omega$ , indicating that the  $\alpha$ -FeOOH addition decreased the anode ohmic resistance and facilitated the charge transfer of bioelectrochemical reactions. The CPE (related with the capacitance) increased from  $3.0 \times 10^{-5} \Omega^{-1} s^N cm^{-2}$  (the control) as follows:  $4.5 \times 10^{-5} \Omega^{-1} s^N cm^{-2}$  (7.5%  $\alpha$ -FeOOH added),  $5.0 \times 10^{-5} \Omega^{-1} s^N cm^{-2}$  (2.5%  $\alpha$ -FeOOH added), and  $5.5 \times 10^{-5} \Omega^{-1} s^N cm^{-2}$  (5.0%  $\alpha$ -FeOOH added). The value of  $N$  for each



**Fig. 4.** Nyquist plots of anodes with different  $\alpha$ -FeOOH contents.

**Table 1**  
Fitting results of anodes with different  $\alpha$ -FeOOH contents according to Nyquist plots.

$\alpha$ -FeOOH content	0 (control)	2.5%	5.0%	7.5%
$R_s (\Omega)$	10.2	7.7	7.6	8.4
$R_{ct} (\Omega)$	26.2	25.6	16.6	16.8
$Q_{dl} (10^{-5} \Omega^{-1} s^N cm^{-2})$	3.0	5.0	5.5	4.5
$W (\Omega s^{-1/2})$	0.47	0.42	0.42	0.46
$N$	0.59	0.56	0.54	0.55

anode is close to 0.5, suggesting the existence of Warburg type impedance  $Z_w$ . Here  $Z_w$  is related to the electron or substrate migration on the surface of the anode, and the Warburg element is given by [32]

$$Z_w = \frac{W}{\sqrt{j\omega}} \quad (3)$$

$$W = \frac{RT}{n^2 F^2 A c \sqrt{De}} \quad (4)$$

Where  $j$  is the imaginary unit ( $j = \sqrt{-1}$ ),  $\omega$  is the angular frequency ( $\text{rad s}^{-1}$ ),  $W$  is the Warburg parameter in units of  $\Omega s^{-1/2}$ ,  $R$  is the gas constant ( $8.314 \text{ J mol}^{-1} \text{ K}^{-1}$ ),  $T$  is the absolute temperature (K),  $n$  is the number of electrons transferred,  $F$  is the Faraday constant ( $96,485 \text{ C mol}^{-1}$ ),  $A$  is the geometric electrode area ( $\text{m}^2$ ),  $c$  is the electrolyte concentration ( $\text{mol L}^{-1}$ ), and  $De$  is the effective diffusivity on the anode.  $A$ ,  $c$  and  $n$  can be considered roughly constant. The equations above show that the decrease in  $W$  is inversely proportional to the increase of  $De$ . In this study, the addition of 2.5% and 5.0%  $\alpha$ -FeOOH decreased  $W$  from 0.47 to 0.42  $\Omega s^{-1/2}$  (Table 1), indicating that the diffusion condition ( $De$ ) was promoted. However, the  $W$  returned to 0.46  $\Omega s^{-1/2}$  with further increment to 7.5% in  $\alpha$ -FeOOH content, which was consistent with the power density curve in context, possibly due to the suppression of biogenic Fe(II) adsorbed on the goethite which could result in the diffusion problem of electron donor and interfere the electron transfer between the c-Ctys protein and the oxide surface [33].

According to the decrease of  $R_{ct}$  after  $\alpha$ -FeOOH addition, it was confirmed that the  $\alpha$ -FeOOH in anode can substantially enhance the EET. Comparing the data of 5.0% and 7.5%  $\alpha$ -FeOOH added anodes in Table 1, it was clearly showed that the dominant

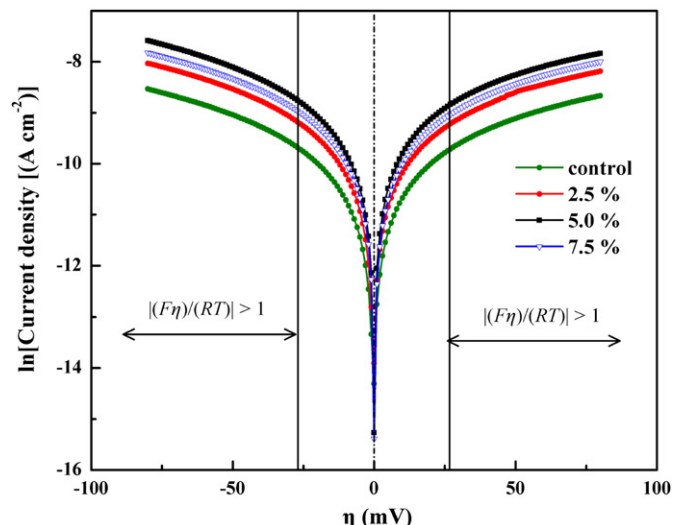


**Fig. 5.** Tafel curves of anodes with different  $\alpha$ -FeOOH contents.

differences were the ohmic resistance ( $R_s$ ), the CPE ( $Q_{dl}$ ) and the Warburg parameter ( $W$ ), not the charge transfer resistance ( $R_{ct}$ ), indicating that the over addition of  $\alpha$ -FeOOH negatively altered the surface conductivity, the capacitance (the capacitance of Fe(III) oxide was important to the anode performance [21]) and the diffusion condition. Further investigation should be conducted to identify the mechanisms in detail.

### 3.3. Electrochemical polarization analysis

The Tafel curves (Fig. 5) were fitted reasonably well ( $R^2 \geq 0.999$ ) at the overpotential of 60–80 mV, where  $|(\mathcal{F}\eta)/(RT)| > 1$  [34]. Since  $(\alpha + \beta) = n$ , the  $n$  value obtained is similar (0.9) and close to 1, indicating that one electron reaction was the rate determining step. Based on the value of  $n$ , the slopes ( $b_a$  and  $b_c$ ) and electron transfer coefficient ( $\alpha$  and  $\beta$ ) of anodic and cathodic reaction are listed in Table 2. Tafel slope is negatively proportional to the electron transfer coefficient. A higher oxidative slope ( $b_a$ ) was observed in Tafel analysis than the reductive slope ( $b_c$ ) for MFC anode, corresponding to a lower oxidative transfer coefficient ( $\alpha$ ) than the reductive transfer coefficient ( $\beta$ ). This is an evidence for the stronger oxidative activity for the anode than the cathode. Due to the logarithmic relation, polarization depends more on Tafel intercept ( $a$ ) than on parameter  $b$  with the value of polarization at the unit current density. Table 2 showed that the  $a$  value of the  $\alpha$ -FeOOH added anodes decreased comparing with that of the control, indicating that the addition of  $\alpha$ -FeOOH alleviated the activation loss. This result was consistent with that obtained in RDAP analysis. It was clearly showed that MFC operated with  $\alpha$ -FeOOH content of 5.0% had the highest  $i_0$  of  $13.3 \times 10^{-5} \text{ A cm}^{-2}$  and KA of 2.5, while both of  $i_0$  and KA decreased when  $\alpha$ -FeOOH contents were 7.5% ( $i_0 = 10.9 \times 10^{-5} \text{ A cm}^{-2}$  and KA = 2.0) and 2.5% ( $i_0 = 9.4 \times 10^{-5} \text{ A cm}^{-2}$  and KA = 1.7). The lowest  $i_0$  of  $5.4 \times 10^{-5} \text{ A cm}^{-2}$  was obtained in the control. The tendency observed in kinetic activity was in fair agreement with the MFC power generation, further confirmed that the addition of  $\alpha$ -FeOOH could promote the EET. Comparing with previous results, the maximum KA obtained here is 89% higher than 1.32 reported in  $\text{Fe}_3\text{O}_4/\text{AC}/\text{SSM}$  composite anode [21], and 14% higher than 2.2 of  $\text{Fe}_3\text{O}_4/\text{ceramic-graphite}$  composite electrode [8]. The differences are probably due to the characteristics of different Fe oxides. These results show that the  $\alpha$ -FeOOH can be a good choice as an improver in anode.

CV, particularly, low scan rate cyclic voltammetry (LSCV), which favored steady-state condition for the interfacial electron transfer between the bacteria and the electrode [35], was used to investigate the oxidation and reduction behavior of different anodes. The voltammetric wave (Fig. 6A) shows that the peak currents (with the point at  $\text{DCV} = 0$ ) of different anodes from the highest to the lowest were 5.3 mA (5.0%  $\alpha$ -FeOOH), 5.2 mA (7.5%  $\alpha$ -FeOOH), 5.0 mA (2.5%  $\alpha$ -FeOOH) and 4.9 mA (the control). According to DCV showed in Fig. 6B, the oxidation current generated by stable-state biological

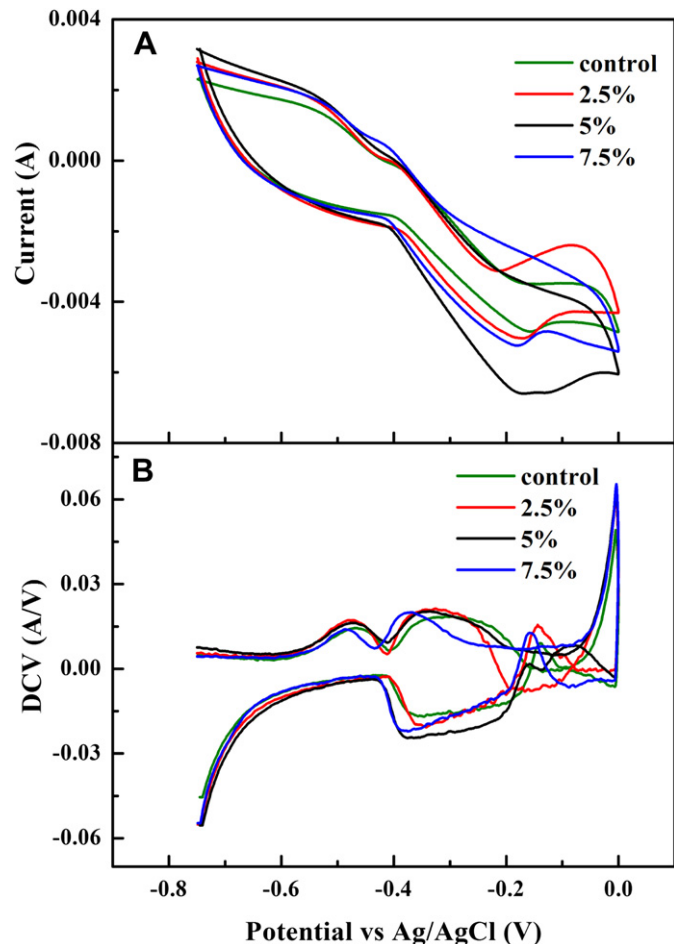


**Fig. 6.** Cyclic voltammetry (A) and first derivative cyclic voltammetry (B) of MFCs with different  $\alpha$ -FeOOH contents.

oxidation of acetate rapidly rose at potential  $-0.43 \text{ V}$  (5.0% and 7.5%  $\alpha$ -FeOOH added anodes) or  $-0.41 \text{ V}$  (2.5%  $\alpha$ -FeOOH added anodes and the control) and reached limiting currents at the potential of  $-0.2 \text{ V}$  (vs. Ag/AgCl). The significant increase in current reflects that more amounts of electrons are involved in charge transfer when  $\alpha$ -FeOOH was added, accounting for the acceleration in EET as illustrated by the EIS and Tafel analysis mentioned above. Unfortunately, no distinct oxidation-reduction peak of Fe was observed in these curves, probably due to the effect of irregular surface of carbon anode and the relative low amount of Fe on the anode surface. As the ammonia treatment of anodes, we have found that tiny amount of N increase on the surface of carbon mesh (N/C from 2.6% to 4.6%) resulted in 14% increase in power density [10]. Thus, it is interesting that the relative low increase of surface element on anode brings an obvious enhancement of the performance. More fundamental research works should be performed in this area in the future.

## 4. Conclusions

The addition of  $\alpha$ -FeOOH enhanced the performance of the anode, with the maximum power density increased by 36% from  $508 \pm 40 \text{ mW m}^{-2}$  (the control) to  $693 \pm 20 \text{ mW m}^{-2}$  (5.0%  $\alpha$ -FeOOH added). Increase or decrease of the  $\alpha$ -FeOOH content to 2.5% or 7.5% resulted in relative lower power outputs. Polarization kinetics and charge transfer resistance analysis demonstrate that the extracellular electron transfer between bacteria and the

**Table 2**  
Kinetic parameters of anodes with different  $\alpha$ -FeOOH contents from Tafel plots.

$\alpha$ -FeOOH content	0 (control)	2.5%	5.0%	7.5%
$n$	0.89	0.89	0.90	0.90
Electron transfer coefficient	$\alpha$ 0.43 $\beta$ 0.47	$\alpha$ 0.40 $\beta$ 0.49	$\alpha$ 0.41 $\beta$ 0.49	$\alpha$ 0.42 $\beta$ 0.48
Tafel slope ( $\text{V dec}^{-1}$ )	$b_a$ 0.07 $b_c$ 0.06	$b_a$ 0.07 $b_c$ 0.06	$b_a$ 0.07 $b_c$ 0.06	$b_a$ 0.07 $b_c$ 0.06
Tafel intercept (V)	$a_a$ 0.67 $a_c$ 0.56	$a_a$ 0.67 $a_c$ 0.56	$a_a$ 0.64 $a_c$ 0.52	$a_a$ 0.63 $a_c$ 0.55
$i_0 (10^{-5} \text{ A cm}^{-2})$	5.4	9.4	13.3	10.9
KA	1.0	1.7	2.5	2.0

electrode was enhanced by  $\alpha$ -FeOOH addition. However, the possible resistances from surface conductivity, diffusion and the decrease of capacitance resulted in the decay of performance when  $\alpha$ -FeOOH was excessive. Since the 5.0%  $\alpha$ -FeOOH added anode had a high kinetic activity of 2.5,  $\alpha$ -FeOOH has been found to be a good choice as an anodic promoter for the future application.

## Acknowledgments

This research was supported by National Natural Science Foundation of China (NSFC, Nos. 21107053 and 51208352).

## References

- [1] X. Wang, Y.J. Feng, H. Lee, Water Sci. Technol. 57 (2008) 1117–1121.
- [2] H. Liu, S. Grot, B.E. Logan, Environ. Sci. Technol. 39 (2005) 4317–4320.
- [3] X.X. Cao, X. Huang, P. Liang, K. Xiao, Y.J. Zhou, X.Y. Zhang, B.E. Logan, Environ. Sci. Technol. 43 (2009) 7148–7152.
- [4] K.S. Jacobson, D.M. Drew, Z. He, Environ. Sci. Technol. 45 (2011) 4652–4657.
- [5] A. Shantaram, H. Beyenal, R. Raajan, A. Veluchamy, Z. Lewandowski, Environ. Sci. Technol. 39 (2005) 5037–5042.
- [6] F. Li, Y. Sharma, Y. Lei, B. Li, Q. Zhou, Appl. Biochem. Biotechnol. 160 (2010) 168–181.
- [7] C.H. Feng, L. Ma, F.B. Li, H.J. Mai, X.M. Lang, S.S. Fan, Biosens. Bioelectron. 25 (2010) 1516–1520.
- [8] D.A. Lowy, L.M. Tender, J.G. Zeikus, D.H. Park, D.R. Lovley, Biosens. Bioelectron. 21 (2006) 2058–2063.
- [9] T. Zhang, C.Z. Cui, S.L. Chen, X.P. Ai, H.X. Yang, S. Ping, Z.R. Peng, Chem. Commun. (2006) 2257–2259.
- [10] X. Wang, S.A. Cheng, Y.J. Feng, M.D. Merrill, T. Saito, B.E. Logan, Environ. Sci. Technol. 43 (2009) 6870–6874.
- [11] H.M. Wang, M. Davidson, Y. Zuo, Z.Y. Ren, J. Power Sources 196 (2011) 5863–5866.
- [12] A. Okamoto, K. Hashimoto, R. Nakamura, Bioelectrochemistry 85 (2012) 61–65.
- [13] L.A. Shi, D.J. Richardson, Z.M. Wang, S.N. Kerisit, K.M. Rosso, J.M. Zachara, J.K. Fredrickson, Environ. Microbiol. Rep. 1 (2009) 220–227.
- [14] R. Nakamura, F. Kai, A. Okamoto, G.J. Newton, K. Hashimoto, Angew. Chem. Int. Ed. 48 (2009) 508–511.
- [15] Y.J. Xiong, L. Shi, B.W. Chen, M.U. Mayer, B.H. Lower, Y. Londer, S. Bose, M.F. Hochella, J.K. Fredrickson, T.C. Squier, J. Am. Chem. Soc. 128 (2006) 13978–13979.
- [16] S.K. Lower, M.F. Hochella, T.J. Beveridge, Science 292 (2001) 1360–1363.
- [17] S. Kato, R. Nakamura, F. Kai, K. Watanabe, K. Hashimoto, Environ. Microbiol. 12 (2010) 3114–3123.
- [18] K. Richter, M. Schicklberger, J. Gescher, Appl. Environ. Microbiol. 78 (2012) 913–921.
- [19] T. Mehta, M.V. Coppi, S.E. Childers, D.R. Lovley, Appl. Environ. Microbiol. 71 (2005) 8634–8641.
- [20] J.Y. Ji, Y.J. Jia, W.G. Wu, L.L. Bai, L.Q. Ge, Z.Z. Gu, Colloid Surf. A 390 (2011) 56–61.
- [21] X. Peng, H. Yu, X. Wang, Q. Zhou, S. Zhang, L. Geng, J. Sun, Z. Cai, Bioresour. Technol. 121 (2012) 450–453.
- [22] L. Xiao, J. Damien, J.Y. Luo, H.D. Jang, J.X. Huang, Z. He, J. Power Sources 208 (2012) 187–192.
- [23] Y. Qiao, S.J. Bao, C.M. Li, X.Q. Cui, Z.S. Lu, J. Guo, ACS Nano 2 (2008) 113–119.
- [24] Y.Z. Fan, S.T. Xu, R. Schaller, J. Jiao, F. Chaplen, H. Liu, Biosens. Bioelectron. 26 (2011) 1908–1912.
- [25] N.A.S. Webster, M.J. Loan, I.C. Madsen, R.B. Knott, J.A. Kimpton, Hydrometallurgy 109 (2011) 72–79.
- [26] M. Mozaffari, M. Taheri, J. Amighian, J. Magn. Magn. Mater. 321 (2009) 1285–1289.
- [27] H. Dong, H. Yu, X. Wang, Q. Zhou, J. Feng, Water Res. 46 (2012) 5777–5787.
- [28] H. Liu, B.E. Logan, Environ. Sci. Technol. 38 (2004) 4040–4046.
- [29] X. Wang, Z. Cai, Q.X. Zhou, Z.N. Zhang, C.H. Chen, Biotechnol. Bioeng. 109 (2012) 426–433.
- [30] S.A. Cheng, D.F. Xing, D.F. Call, B.E. Logan, Environ. Sci. Technol. 43 (2009) 3953–3958.
- [31] J. Menicucci, H. Beyenal, E. Marsili, R.A. Veluchamy, G. Demir, Z. Lewandowski, Environ. Sci. Technol. 40 (2006) 1062–1068.
- [32] G.H. Xu, C. Zheng, Q. Zhang, J.Q. Huang, M.Q. Zhao, J.Q. Nie, X.H. Wang, F. Wei, Nano Res. 4 (2011) 870–881.
- [33] C.X. Liu, S. Kota, J.M. Zachara, J.K. Fredrickson, C.K. Brinkman, Environ. Sci. Technol. 35 (2001) 2482–2490.
- [34] V.S. Bagotsky, Fundamentals of Electrochemistry, in: Polarization of Electrodes John Wiley and Sons, 2006, pp. 79–99.
- [35] K. Katuri, M.L. Ferrer, M.C. Gutiérrez, R. Jiménez, F. del Monte, D. Leech, Energy Environ. Sci. 4 (2011) 4201–4210.